JOURNAL OF MATERIALS SCIENCE 21 (1986) 529–535

Phase transformation and age-hardening of Au–Cu–Pd ternary alloys

MICHIO OHTA, TAKANOBU SHIRAISHI, MASAJI YAMANE
Department of Dental Materials Engineering, Faculty of Dentistry, Kyushu University, Fukuoka 812, Japan

Phase transformations in Au–Cu–Pd single-phase alloys were studied. Age-hardening of the alloys examined was attributed to the formation of fine domains of long-range ordered (LRO) AuCuI type lattice in the interior of the grain. Prolonged ageing caused formation of large LRO domains of single variant at the grain boundary or microtwinning of LRO in the interior of the grain, depending on the ordering rate of the alloy. The electron–atom ratio (*e*/*a*) of the alloy and the axial ratio (*c*/*a*) of the ordered lattice seemed to play a part in the phase transformation behaviour in this alloy system. The effectiveness of rhodium addition on the grain refining was proved experimentally. These results will be helpful in developing low nobility and high corrosion resistant dental alloys.

1. Introduction

Dental alloys for the oral environment have to be those possessing chemical stability and biocompatibility. Enough strength for each purpose is also required. Among the wide variation of commercial dental gold alloys, highly noble and age-hardenable ones meet the above-mentioned requirements.

Examination of dental gold alloys by a potentiodynamic technique [1, 2] shows that nobility (the total amount of gold and platinum group metals) is a dominant factor in determining corrosion resistance, and that control of microstructure can improve corrosion resistivity. According to the above criteria, nobility above 55 at % [1] and single-phase structure [3] are preferred. So far as a single phase is concerned, only disorder-to-order reaction, not precipitation, is adopted as the age-hardening mechanism.

The principal constituents of dental gold alloys are gold, copper and silver. Age-hardening is mainly due to the formation of AuCu ordered phase [4, 5]. As is evident from the Au–Cu–Ag ternary phase diagram [6–8], most of the AuCu ordered phase region in overlapped with a two-phase (silver- and copper-rich) coexisting region; that is, the equilibrium phases of most dental gold alloys at low temperatures are the ordered AuCu and silver-rich disordered phases. The existence of a silver-rich phase is responsible for the tarnish of gold alloys because of chloride formation [8, 9].

It can be seen from the Au–Cu–Pd ternary phase diagram [10] that a wide compositional range of the AuCu type ordered phase exists without any other phase. According to studies on the phase transformations of stoichiometric AuCu [8], CuPd [11, 12] and AuCu–$Cu_{0.6}Pd_{0.4}$ pseudo-binary alloys [13], the following are suggested;

(a) Ordering in the $Cu_{0.6}Pd_{0.4}$ alloy (referred as CuPd hereafter) is discontinuous, and the fully ordered structure is characterized by a large size grain boundary product of long-range ordered (LRO) phase (a single variant of LRO). On the other hand, stoichiometric AuCu exhibits continuous ordering.

(b) The electron–atom ratio (*e*/*a*) of the alloy influences the formation of fine LRO domains, in other words the formation of short-range order(SRO).

This study is intended to develop dental gold alloys of the Au–Cu–Pd system with high corrosion resistance which have AuCuI type ordered single phase and fine uniform microstructure.

2. Materials and methods

Chemical compositions of the alloys examined are shown in Table I and also in the isothermal section (at 350° C) of the Au–Cu–Pd system (Fig. 1). Gold and copper (99.99% pure) and 35.0% Au–35.9% Cu–29.1% Pd alloy were weighed to obtain 5 g casts. They were melted and cast to parallelepiped specimens (3 mm × 1.5 mm × 23 mm) in an argon atmosphere using a high-frequency induction furnace. Besides as-cast specimens, homogenized specimens were prepared by cold rolling (to about half its original thickness) and annealing (at 800° C for 2 h) the as-cast parallelepipeds. Sheets of 0.1 mm thick were also prepared by alternate rolling and annealing.

These specimens were solution treated at 600° C for 30 min followed by iced-brine quenching. Isothermal ageing was performed at 300° C. Hardness tests were made using a diamond pyramid hardness indenter with a 500 g load. The Vickers hardness was obtained as the average of five indentations. Structural changes by ageing were examined by optical and transmission electron microscopy at the ageing time corresponding to the hardness peak, and also to the overaged state. 3 mm diameter discs were punched out of the heat-treated sheets. They were electrothinned by a double-jet polish technique in a solution of 35 g of CrO_3,

© *1986 Chapman and Hall Ltd.*

TABLE I Chemical compositions of alloys used

Alloy	Composition (at %)			
	Au	Cu	Pd	Ag
I	37.1	51.9	11.0	–
I–5	34.5	49.0	11.5	5.0
II	46.0	43.0	11.0	–
III	26.1	63.2	10.7	–

200 ml of CH_3COOH and 10 ml of distilled water. The electron microscope used was a JEM–1000 (HVEM Laboratory, Kyushu University) operating at 1000 kV.

X-ray diffraction study was carried out on the filed and appropriately heat-treated powder specimens using nickel-filtered Cu$K\alpha$ radiation.

3. Results and discussion

3.1. Phase transformation behaviour

Since age-hardening is caused by structural changes from the non-equilibrium to the equilibrium state, it is necessary to clarify the stable phase(s) of the alloy and the changes to the final state at the ageing temperature. Experiment for such purposes should be carried out using homogenized specimens, not as-cast alloys.

X-ray diffraction patterns of Alloys I, II and III aged at 300° C for 30 000 min are demonstrated in Fig. 2. These patterns indicate that the stable phase of these alloys at 300° C is an AuCuI type ordered phase. On the other hand, precipitation of a silver-rich (α_2 phase) from the AuCuI type occurs in Alloy I–5 which contains 5% Ag, as shown in Fig. 3.

Structural changes by isothermal ageing was examined by transmission electron microscopy and selected-area electron diffraction. Fig. 4a is a selected-area diffraction pattern taken from Alloy I aged at 300° C for 10 min. Analysis of the pattern proved that this pattern is an overlapping of three variants of the AuCuI type superlattice. Fig. 4b is a dark-field image taken by using the 0 0 1 superlattice spot. AuCuI type ordered domains are observed to form along [0 1 1] and [0 $\bar{1}$ 1] directions of the matrix. These features in Fig. 4 are similarly observed at the early ageing stage of every alloy tested in this study, and are quite similar to those in the stoichiometric AuCu alloy [8].

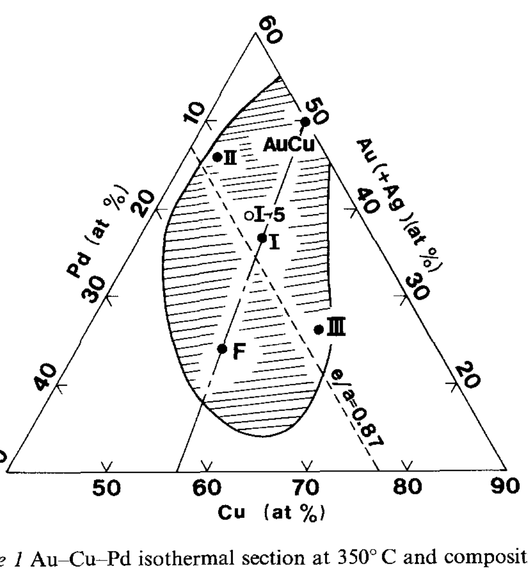

Figure 1 Au–Cu–Pd isothermal section at 350° C and composition of alloys studied. Hatched area is AuCuI type single-phase region.

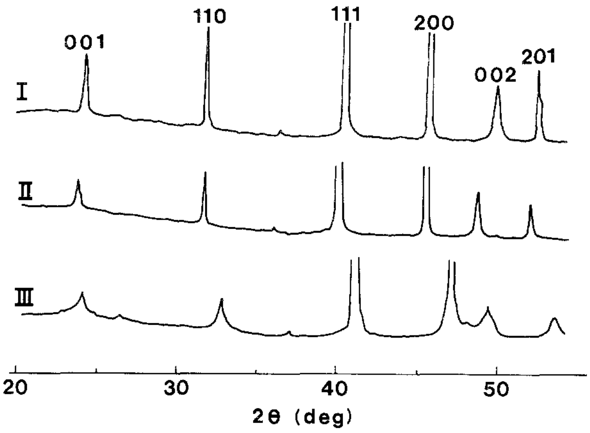

Figure 2 X-ray diffraction patterns of Alloys I, II and III aged at 300° C for 30 000 min.

Fig. 5 is a bright-field image of Alloy II aged for 1000 min. Microtwinning of AuCuI type ordered phase covered whole grains, by analogy with the stoichiometric AuCu alloy. Fig. 6a is a bright-field image of Alloy I aged for 1000 min, and Fig. 6b is a selected-area diffraction pattern taken from the region in the circle in Fig. 6a. This pattern corresponds to one of three variants of the AuCuI superlattice. It is proved from the above observations that prolonged ageing of Alloy I causes the formation of course domains of AuCuI type ordered phase at grain boundaries. This feature is quite different from the stoichiometric AuCu alloy but quite similar to those in CuPd [12] and CuPd–AuCu pseudo-binary alloys [13]. As shown in Fig. 6a, twinning occurs in some large domains.

Figs. 7a and b are bright-field images of alloy I–5 aged for 100 and 1000 min, respectively. By prolonged ageing, the grain boundary product was converted from coarse domains of AuCuI type ordered phase into nodules which consist of AuCuI type superlattice and silver-rich α_2 disordered fcc. These observations coincide with the results obtained by X-ray diffraction (Fig. 3).

Fig. 8 is a bright-field image of Alloy III aged at 300° C for 30 000 min. Despite the long ageing time,

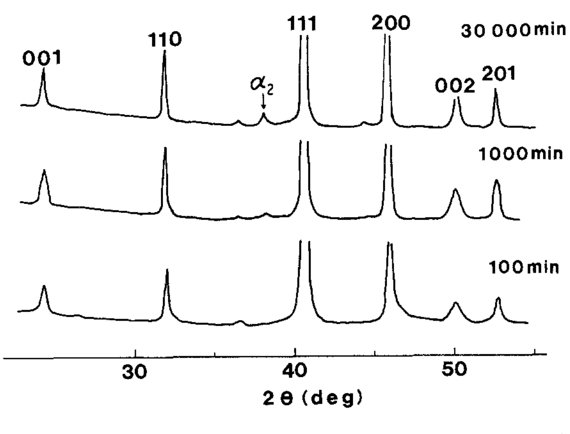

Figure 3 Change in X-ray diffraction pattern of Alloy I–5 by ageing at 300° C.

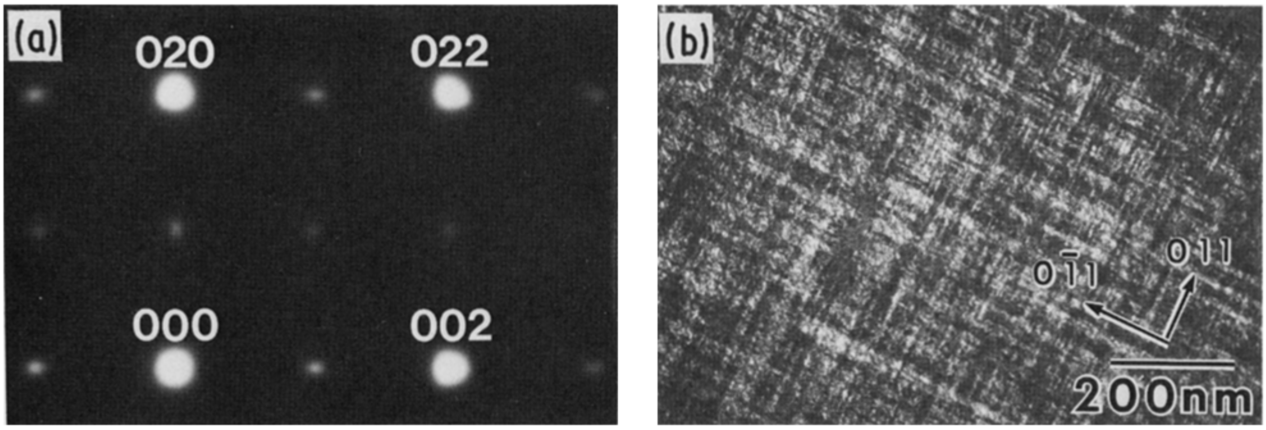

Figure 4 (a) Selected area diffraction pattern and (b) 0 0 1 dark-field image of Alloy I aged at 300° C for 10 min.

the contrast in the matrix is almost the same as that in Alloy I aged for only 10 min (Fig. 4b) and the amount of grain boundary product seems to be smaller than that in Alloy I–5 aged for 100 min. These facts suggest that the ordering rate in this alloy is extremely slow in comparison with other alloys.

Fig. 9a to d are optical micrographs of Alloys I, II, III and I–5, respectively, aged for 5000 min. In Alloy I, the original grain was refined by the replacement of grain boundary product. In Alloy I–5, the grain boundary product was apparently nodular. On the other hand, no clear difference can be seen between pre-ageing and post-ageing in Alloys II and III. However, twins and striations caused by ordering were observed in the grain interior of Alloy II. The above observations confirm the conclusions on the phase transformation process which were obtained by transmission electron microscopy.

The above-mentioned phase transformation processes are summarized below. Results on stoichiometric AuCu [8] CuPd [12] and Cu–21.34 at % Pd–23.86 at % Cu (Alloy F) [13] are also shown for comparison.

CuPd: $\rightarrow \mathrm{SRO}^{\mathrm{I}} \rightarrow \mathrm{SRO}^{\mathrm{I}} + \mathrm{LRO}^{\mathrm{B}}(\mathrm{SV})$
$\rightarrow \mathrm{LRO}^{\mathrm{B}}(\mathrm{SV})$

F: $\rightarrow \mathrm{SRO}^{\mathrm{I}} \rightarrow \mathrm{LRO}^{\mathrm{I}} \rightarrow \mathrm{LRO}^{\mathrm{I}} + \mathrm{LRO}\ (\mathrm{SV})^{\mathrm{B}}$
$\rightarrow \mathrm{LRO}\ (\mathrm{SV})^{\mathrm{B}}$

AuCu: $\rightarrow \mathrm{LRO}^{\mathrm{I}} \rightarrow \mathrm{LRO}^{\mathrm{I}}$ (twin)

II: $\rightarrow \mathrm{LRO}^{\mathrm{I}} \rightarrow \mathrm{LRO}^{\mathrm{I}}$ (twin)

I: $\rightarrow \mathrm{LRO}^{\mathrm{I}} \rightarrow \mathrm{LRO}^{\mathrm{I}} + \mathrm{LRO}^{\mathrm{B}}\ (\mathrm{SV})$
$\rightarrow \mathrm{LRO}^{\mathrm{B}}\ (\mathrm{SV})$

III: $\rightarrow \mathrm{LRO}^{\mathrm{I}} \rightarrow \mathrm{LRO}^{\mathrm{I}} + \mathrm{LRO}^{\mathrm{B}}\ (\mathrm{SV})$
$\rightarrow \mathrm{LRO}^{\mathrm{B}}\ (\mathrm{SV})$

I-5: $\rightarrow \mathrm{LRO}^{\mathrm{I}} \rightarrow \mathrm{LRO}^{\mathrm{I}} + \mathrm{LRO}^{\mathrm{B}}$
$\rightarrow \mathrm{LRO}^{\mathrm{I}} + \mathrm{nodule}^{\mathrm{B}}$

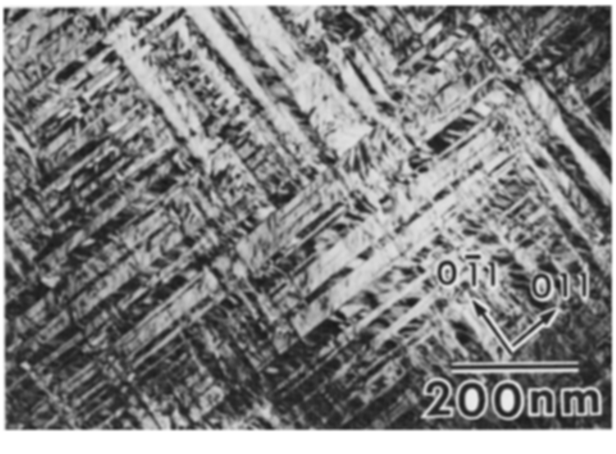

Figure 5 Bright-field image of Alloy II aged at 300° C for 1000 min.

where I and B mean that new phase appears in the grain interior and at the grain boundary, respectively, and SV is the abbreviation for single variant. Accordingly, $\mathrm{LRO}^{\mathrm{B}}$ (SV) means that a long-range ordered phase of single variant forms at the grain boundary. Since the phase transformation process of each alloy described above is constructed with some elemental reactions, the alloys can be classified as follows according to the manner in which each elemental reaction occurs or not:

(a) SRO is formed in the grain interior, (CuPd, F) or not (others). This problem is related to the electron–atom ratio (*e*/*a*) of the alloy. The results of our study on the phase transformation process of CuPd–AuCu pseudo-binary alloys [13] suggest that SRO is formed at the initial stage of ageing in the alloys with $e/a < 0.87$. The values of *e*/*a* for all the alloys studied were calculated to be 0.89 from the values of 1 and 0 for the number of conduction atoms of gold and copper, respectively. This means that SRO does not form in the alloys studied and that, in other words, fine domains of LRO form at the initial stage of ageing.

(b) Nodules form at grain boundaries (I–5) or not (others). This problem simply depends on the amount of silver added to the alloy. In the case where the amount of silver exceeds the solubility limit, precipitation of a silver-rich phase occurs, that is, nodules appear at the grain boundary. It is clear that the solubility of silver in Alloy I is less than 5%.

(c) Grain boundary reaction does not occur (AuCu, II) or occurs (others). This problem seems to depend on the rate of ordering of the alloy. In general, long-range diffusion of atoms is required for the precipitation of a phase. On the other hand, ordering is attained by short-range diffusion. Since a considerable

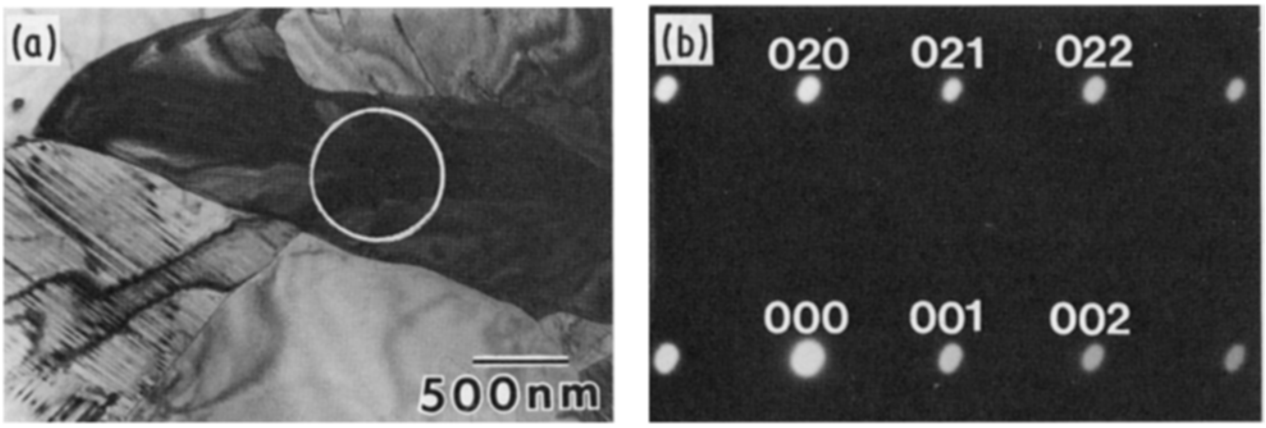

Figure 6 (a) Bright-field image and (b) selected-area diffraction pattern of Alloy I aged at 300° C for 1000 min.

number of quenched-in vacancies are expected to be introduced by quenching after disordering heat treatment, SRO (CuPd and F) or fine domains of LRO (others) are formed by the consumption of excess vacancies. After excess vacancies are annihilated, thermal equilibrium vacancies contribute to the growth of ordered domains to favour ordering. However, in a case where the growth of domains is not easy for some reason, ordering has to proceed by an easier way, i.e. formation of new domains at the grain boundary by the mechanism of bounary diffusion [12].

Two factors can affect the difficulty of domain growth in the interior of a grain. One is the decrease in the diffusion rate of AuCu alloy by the addition of the third element. This prediction can be proved by the fact that the ordering rate of AuCu is decreased by the addition of silver [8] or palladium [13]. Another factor is the axial ratio (c/a) of AuCuI type face centred tetragonal (fct) structures. The growth of ordered domains with tetragonal structure accompanies an increase in elastic strain around them. In an alloy with a large value of c/a, ordered domains grow easily and the critical size for a twin nucleus [14] can be attained. This is the case for stoichiometric AuCu and Alloy II. Change in c/a of alloys by ageing (Fig. 10) shows that c/a values of AuCu and Alloy II are larger than for Alloys I and I–5 at any stage of ageing.

The axial ratio of Alloy III is close to unity and the rate of ordering is expected to be extremely slow, as already mentioned. In this alloy, the atomic ratio Cu/Au is 2.42 (Cu/Au for Alloy II is 0.93). Consequently, a large deviation from stoichiometry may be the main reason for the slow ordering rate in this alloy.

3.2. Age-hardening behaviour

Age-hardening curves of Alloys I, II and III at 300° C are shown in Fig. 11. Comparing the curves of homogenized and as-cast specimens, the homogenized specimen is harder than the as-cast one, and the hardening rate of homogenized Alloy II at the early stage of ageing is larger than that of the as-cast one. However, for all alloys, the shape of the curve is not changed essentially by homogenization. Therefore it is reasonable to consider that there is no essential difference in the age-hardening mechanism between as-cast and homogenized alloys.

The results of transmission electron microscopy lead to the conclusion that age-hardening in all the alloys examined is attained by the formation of fine AuCu ordered domains which accompany an elastic strain field. The coarse grain of the boundary product causes drastic softening at 10 min in Alloy I, and the slight decrease in hardness in Alloy II is attributed to microtwinning which causes a slight release of elastic strain.

3.3. Grain refining of as-cast specimens

An optical micrograph of the as-cast structure of

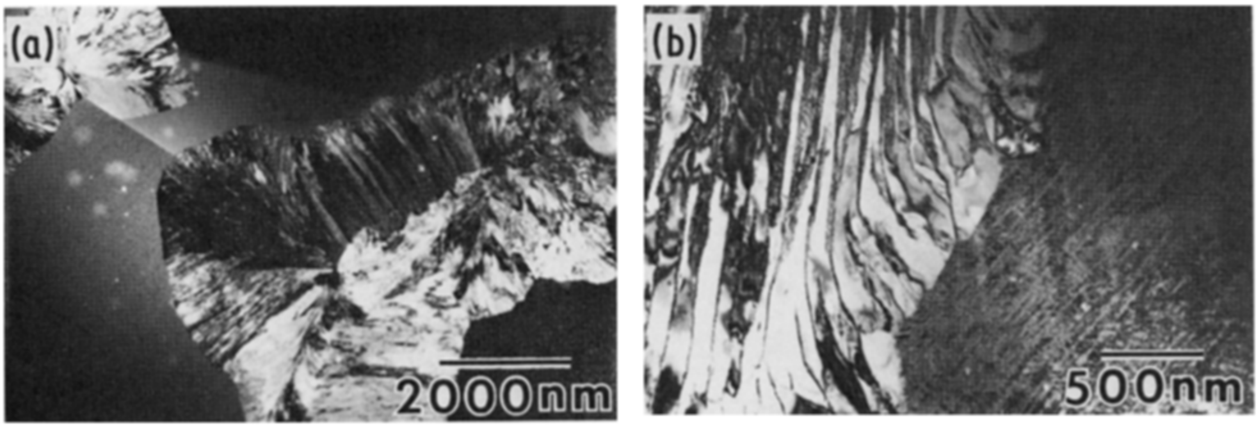

Figure 7 Bright-field images of Alloy I–5 aged at 300° C for (a) 100 min and (b) 1000 min.

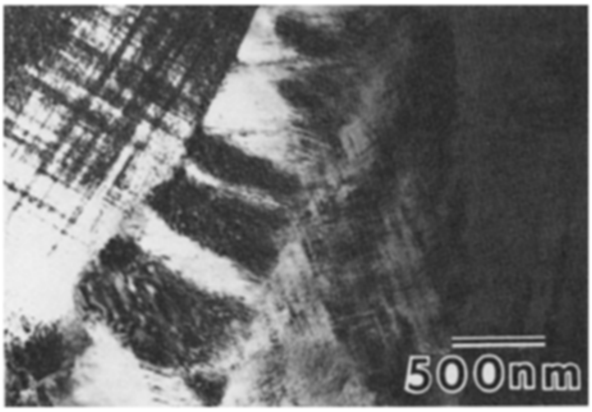

Figure 8 Bright-field image of Alloy III aged at 300° C for 30 000 min.

Alloy II is shown in Fig. 12a. This structure is characterized by coarse grains and dendrititic fine structure, which suggests microsegregation of the constituents. The heterogeneity in grain size and in the distribution of constituents is apparently a serious disadvantage in both the mechanical and chemical properties of an alloy.

In this study, the effect of rhodium addition on grain refinement was examined on Alloys II (richest in gold) and III (richest in copper). As shown in the micrographs of Figs. 12b to d, the grain size of as-cast Alloy II decreased with the amount of rhodium up to 1.9 at %. However, excess addition caused precipitation of a second phase, which is shown in Fig. 13 as white particles.

Fig. 14, which exhibits the relation between the number of grains per unit area and the amount of rhodium added, revealed that rhodium addition has a greater effect on Alloy II than on Alloy III.

Honma and Iijima [15] reported that only 0.005 % Rh addition was effective in the grain refining of silver. They also concluded that this remarkable effect was related to the large value of the equilibrium distribution coefficient (K) of rhodium in the Ag–Rh system. On the basis of the above reasoning and using Ag–Rh [16], Au–Rh [17] and Cu–Rh [18] binary phase diagrams, it is reasonable to speculate that K values for rhodium with gold and copper are much smaller than with silver.

4. Conclusions

Phase transformations in Au–Cu–Pd single-phase

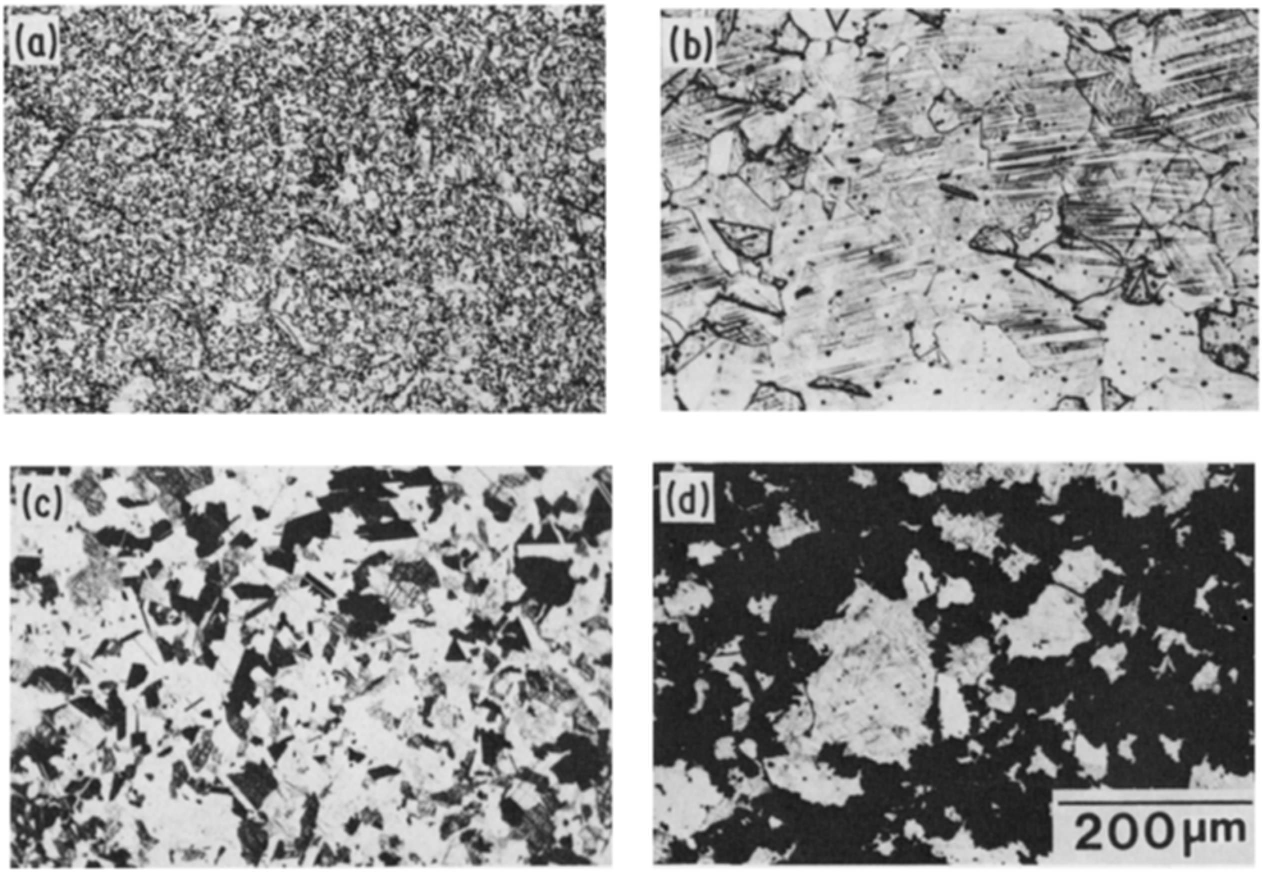

Figure 9 Optical micrographs of Alloys (a) I, (b) II, (c) III and (d) I-5 aged at 300° C for 5000 min.

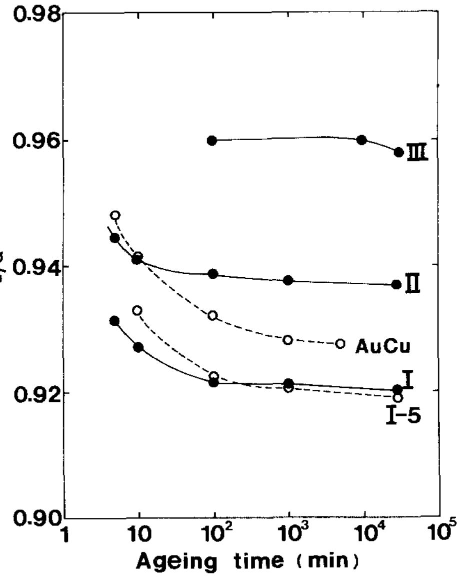

Figure 10 Change in axial ratio (c/a) by ageing at 300° C.

alloys were studied and the following results were obtained, which will be helpful in developing low nobility and high corrosion resistant dental alloys.

1. All alloys of the Au–Cu–Pd ternary system examined in this study exhibited a single phase with ordered AuCuI type structure by the ageing at 300° C. Precipitates of a silver-rich phase appeared at the grain boundary in alloys containing silver.

2. Age-hardening of the alloys studied was attributed to the formation of fine domains of LRO AuCuI type lattice in the interior of the grain.

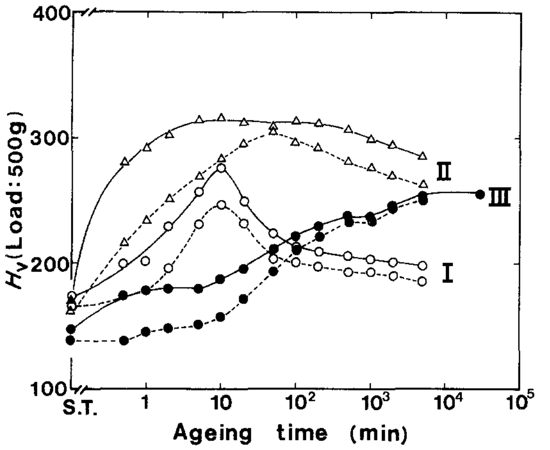

Figure 11 Age-hardening curves of Alloys I, II and III. Solid lines are for homogenized specimens and dashed lines are for as-cast specimens.

3. In alloys in which the ordering rate was slow, large LRO domains of single variant appeared at the grain boundary after prolonged ageing. On the other hand, prolonged ageing caused microtwinning of ordered phase in the grain interior in alloys with a high ordering rate.

4. The axial ratio (c/a) of ordered AuCuI lattice seemed to play a part in the growth rate of fine LRO domains, i.e. in the ordering rate.

5. Rhodium addition to Au–Cu–Pd alloys was effective in grain refinement.

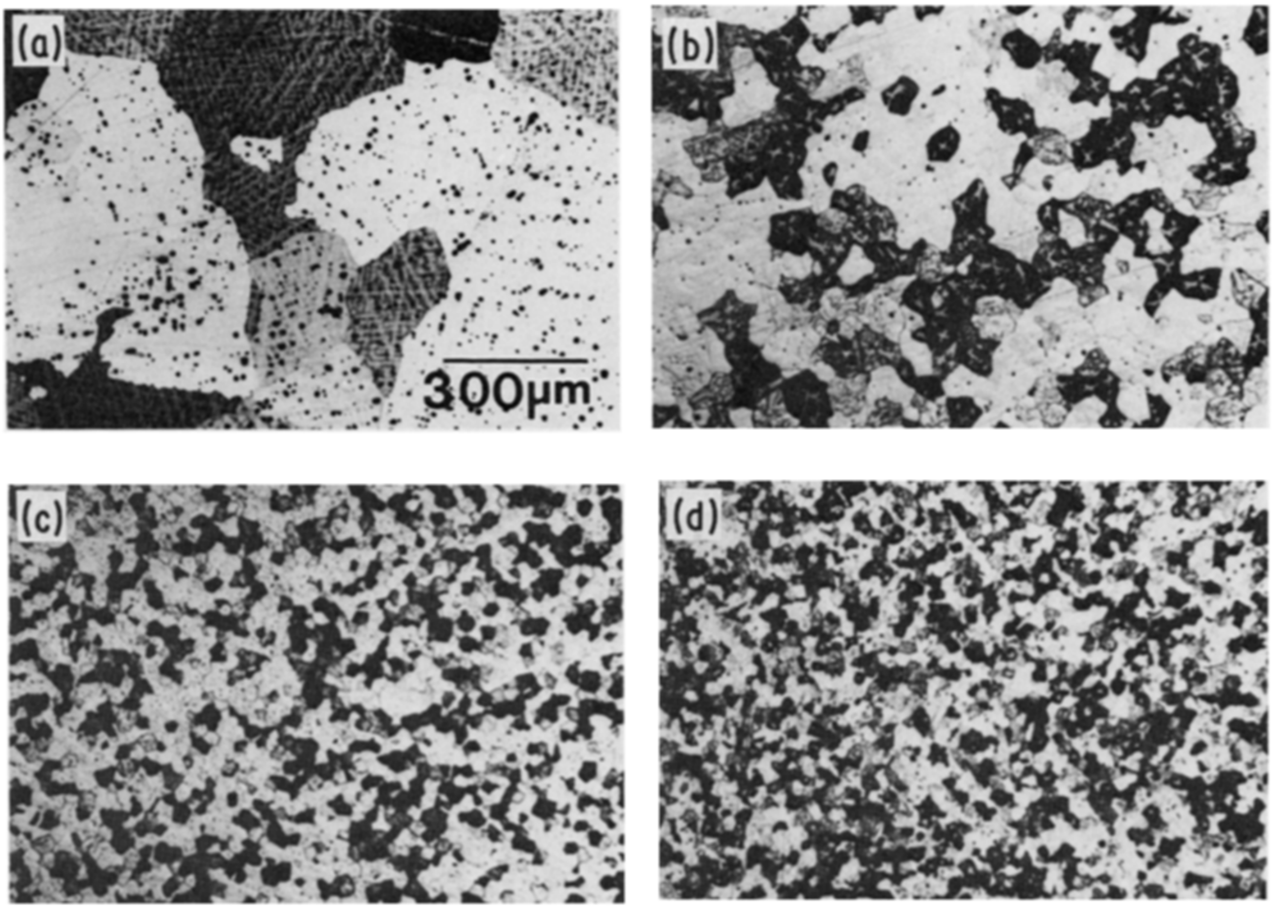

Figure 12 Optical micrographs of as-cast alloy II. Amount of rhodium addition is (a) 0%, (b) 1.25 at %, (c) 1.89 at % and (d) 2.51 at %.

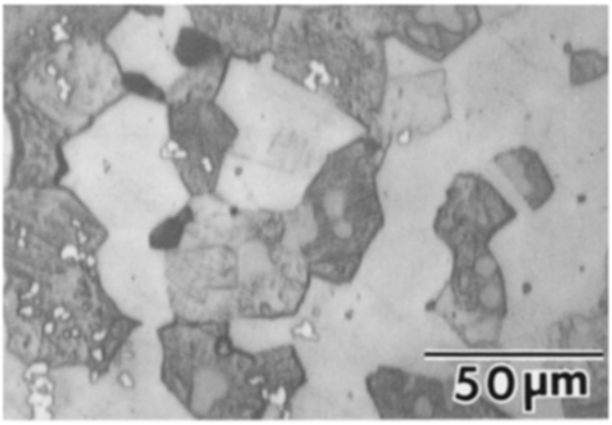

Figure 13 Optical micrograph of as-cast Alloy II containing 2.51 at % Rh (an enlargement of Fig. 12d).

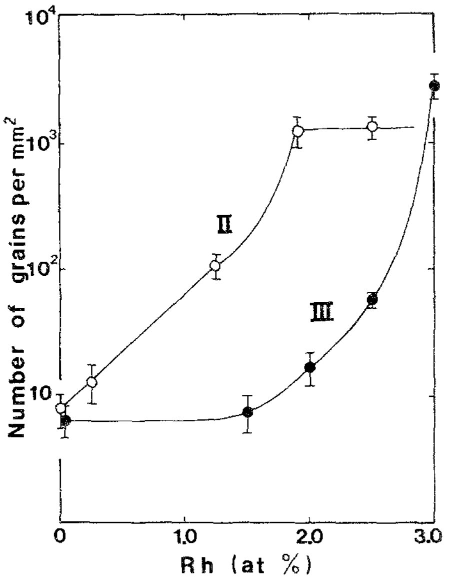

Figure 14 Relation between the number of grains per unit area and the amount of rhodium addition for Alloys II and III.

References

1. R. M. GERMAN, D. C. WRIGHT and R. F. GALLANT, in Proceedings of the 5th International Conference on Precious Metals, Toronto, June 1980, edited by R. O. McGachie and A. D. Bradley (Pergamon Press, Canada, 1981) p. 253.
2. D. L. TREASY and R. M. GERMAN, *Gold Bulletin* **17** (1984) 46.
3. H. HERØ and R. B. JØRGENSEN, *J. Dent. Res.* **62** (1983) 371.
4. K. YASUDA and M. OHTA, *ibid.* **61** (1982) 473.
5. K. YASUDA, K. HISATSUNE and M. OHTA, *Int. Dent. J.* **33** (1983) 11.
6. T. UZUKA, Y. KANZAWA and K. YASUDA, *J. Dent. Res.* **60** (1981) 883.
7. H. YAMAUCHI, H. A. YOSHIMATSU, A. R. FROUHI and D. deFONTAINE, in Proceedings of the 5th International Conference on Precious Metals, Toronto, June 1980, edited by R. O. McGachie and A. D. Bradley (Pergamon Press, Canada, 1981) p. 241.
8. M. OHTA, T. SHIRAISHI and M. YAMANE, *Dent. Mater. J.* **2** (1983) 10.
9. R. M. GERMAN, *Metallography* **14** (1981) 253.
10. E. RAUB und G. WÖRWAG, *Z. Metallkde* **46** (1955) 119.
11. T. SHIRAISHI, *J. Jpn. Soc. Dent. Appar. Mater.* **22** (1981) 119.
12. *Idem, J. Jpn. Inst. Met.* **46** (1982) 245.
13. T. SHIRAISHI, M. OHTA and M. YAMANE, *Dent. Mater. J.* **3** (1985) 193.
14. G. C. KUCZINSKI, R. F. HOCHMAN and M. DOYAMA, *J. Appl. Phys.* **26** (1955) 871.
15. H. HONMA and K. IIJIMA, *J. Jpn. Soc. Dent. Mater. Devices* **2** (1983) 824.
16. R. P. ELLIOT, in "Constitution of Binary Alloys", First Supplement (McGraw-Hill, New York, 1965) p. 18.
17. *Idem*, "Constitution of Binary Alloys", First Supplement (McGraw-Hill, New York, 1965) p. 100.
18. M. HANSEN and K. ANDERKO, in "Constitution of Binary Alloys" (McGraw-Hill, New York, 1958) p. 619.

Received 8 March
and accepted 20 March 1985